

# Mechanistic Pathways of the Hydroxyl Radical Reactions of Quinoline. 1. Identification, Distribution, and Yields of Hydroxylated Products

A. Roxana Nicolaescu,<sup>†,‡,§</sup> Olaf Wiest,<sup>\*,‡,||</sup> and Prashant V. Kamat<sup>\*,†,⊥</sup>

Radiation Laboratory, Department of Chemistry and Biochemistry, and  
Department of Chemical and Biomolecular Engineering, University of Notre Dame,  
Notre Dame, Indiana 46556-0579

Received: November 1, 2004; In Final Form: January 17, 2005

The mechanistic details of the hydroxyl radical-induced transformations of quinoline have been elucidated. The nature and distribution of the final products have provided insight into the preferential attack of the hydroxyl radicals at different sites on the aromatic rings. Hydroxylated products at all of the carbon atoms but one, C2, have been observed and quantified following controlled radiolysis of N<sub>2</sub>O-purged aqueous quinoline solutions. The difference in the growth pattern and the lifetime of the monohydroxylated products under radiolytic conditions, as well as the formation of high-molecular-weight products (e.g., quinoline dimers), shows the complexity of the •OH reaction pathways. The radiolytic yields (*G* values) for the degradation of the quinoline and the formation of the hydroxylated products are calculated in the absence and in the presence of an oxidant, K<sub>3</sub>Fe(CN)<sub>6</sub>. The addition of K<sub>3</sub>Fe(CN)<sub>6</sub> changes only the distribution of the hydroxylated products. These experiments indicate that the nature of the hydroxylated products is determined in the initial addition step of the reaction of the hydroxyl radical with quinoline, whereas the chemistry of the OH adducts is relevant to the distribution of the final products. The discrepancy between the products of  $\gamma$ -radiolysis and the photo-Fenton reaction of quinoline is also discussed.

## Introduction

The hydroxyl radical is a ubiquitous reactive species that has attracted a lot of interest from scientists in a variety of disciplines/fields.<sup>1–11</sup> It is the species responsible for the initiation of the tropospheric oxidation of aromatic compounds.<sup>2,12–15</sup> •OH is also an important reactant in environmental remediation for organic pollutants because it is considered to be one of the main oxidizing species in advanced oxidation processes (AOPs).<sup>3,16–18</sup> The hydroxyl radical is generated during biological oxidative stress<sup>19</sup> and plays a very important role in DNA damage.<sup>1,20</sup> It is believed to be implicated in aging and in the pathogenesis of numerous degenerative or chronic diseases.<sup>21,22</sup> The occurrence of hydroxyl radicals during radiation therapy is a matter of immense concern. Despite the effort to elucidate the mechanisms of the reaction of •OH with organic compounds over the last several decades, the reactivity of the hydroxyl radical has remained complex, and the ambiguities concerning the mechanistic pathways have often lead to conflicting remarks.

In many oxidative processes, mechanistic information was sought on the basis of the analysis of the final hydroxylated products.<sup>7,23,24</sup> The isomer ratios in aromatic hydroxylation are often used as proof of the presence or the absence of the hydroxyl radical.<sup>23–25</sup> Because the hydroxyl radical may not be the only or even the main reactive species produced in many oxidative reactions, the nature and distribution of the products

vary dramatically. Changes in the reaction conditions can also introduce further complexity.<sup>25–27</sup> Conflicting information regarding the exact contribution and role of the hydroxyl radical has hence generated uncertainty about its reactivity and the reaction mechanism. For example, to probe the reactivity of •OH in solutions, many experimental studies use Fenton's reagent (a mixture of ferrous ions and hydrogen peroxide) as the source of free hydroxyl radicals. Although the Fenton reaction is more than a century old,<sup>28</sup> there is still no consensus in the literature about the mechanism and the key intermediates responsible for the oxidation.<sup>29–33</sup> Walling and Johnson<sup>25</sup> reported various isomer ratios of cresols in the hydroxylation of toluene with Fenton's reagent, whereas Eberhardt and co-workers<sup>26</sup> reported different isomer ratios while studying aromatic hydroxylation by radiolysis. Both experimental and theoretical studies have shown that oxidizing species other than the •OH radical can also contribute to the reactivity in the Fenton systems. Buda and co-workers<sup>34</sup> did a theoretical study of the Fenton reaction and suggested that the high-valent ferryl complex Fe(IV)O<sup>2+</sup> is the active intermediate in the oxidation reaction, as proposed in a previous study.<sup>35</sup> The issue of the prevalent mechanism in the Fenton reaction is also of great interest in biological research.<sup>36,37</sup>

The importance of the radiolysis studies in establishing mechanistic details comes from the fact that they represent a clean source for the generation of oxidative radicals whose yields are precisely known. Therefore, the product spectrum observed in  $\gamma$ -radiolysis has been used as a reference by studies interested in the assessment of the mechanistic contribution of •OH radicals during photocatalysis, Fenton reactions, or other AOPs.<sup>38–40</sup>

The present study is part of a larger effort to understand the fundamental aspects of the reaction mechanism of •OH radicals with aromatic compounds. In the present paper (part 1), we

\* Corresponding author. E-mail: pkamat@nd.edu. Web: <http://www.nd.edu/~pkamat>.

<sup>†</sup> Notre Dame Radiation Laboratory.

<sup>‡</sup> Department of Chemistry and Biochemistry.

<sup>§</sup> E-mail: nicolaescu@hertz.rad.nd.edu.

<sup>||</sup> E-mail: owiest@nd.edu.

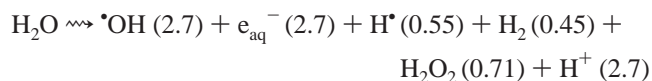
<sup>⊥</sup> Department of Chemical and Biomolecular Engineering.

report our experimental investigation of the mechanistic aspects of the reaction of the hydroxyl radical with quinoline (aqueous solutions) using  $\gamma$ -radiolysis. Quinoline, an N heterocycle, is part of the structure of many antiseptics, antibiotics, and other pharmaceuticals, and it is also used as a raw material and solvent in the manufacture of dyes, herbicides, and paints.<sup>41</sup> Quinoline was chosen in a previous study as a molecular probe used to clarify the mechanism of  $\bullet$ OH oxidation of aromatic pollutants.<sup>42</sup> We started the investigation of the reactivity of  $\bullet$ OH toward quinoline as a first step in understanding the environmental fate of an imidazolinone herbicide, Imazaquin. The reaction of quinoline with  $\bullet$ OH comprises two events: the initial attack leading to the formation of radical species with finite lifetimes (OH adducts) and the transformations of these species to yield the steady-state products. As shown in our earlier pulse radiolysis study,<sup>43</sup> the formation of OH adducts occurs with a diffusion-controlled rate and is completed on the microsecond time scale. However, the decay of these transients is greatly influenced by the medium. To get a snapshot of the initial  $\bullet$ OH attack, the course of the reaction was altered by introducing an oxidant  $-\text{K}_3\text{Fe}(\text{CN})_6-$  into the solution. The presence of such an oxidant ensures fast, quantitative conversion of the OH adducts to the final products. The monohydroxylated products formed upon irradiation of  $\text{N}_2\text{O}$ -saturated solutions of quinoline are identified and quantified in the absence and the presence of  $\text{K}_3\text{Fe}(\text{CN})_6$ , and the results are compared to a previous study of this system<sup>42</sup> in which the hydroxyl radical was generated during the photo-Fenton reaction. These results are complemented by DFT computational studies of the attack of  $\bullet$ OH on quinoline, which are presented separately in the second part of the study.<sup>52</sup>

## Experimental Section

**Chemicals.** Quinoline (Lancaster, 98%) was distilled prior to use; all other reagents and standards were purchased from Aldrich (maximum purity grade, >98%), except tetraethylammonium bromide (Fluka, 98%), tetra-*n*-propylammonium bromide (TCI, 98%), and potassium ferricyanide (Kodak, 99%). The following compounds were prepared and purified by published methods: 3-hydroxyquinoline<sup>44</sup> and quinoline-5,8-dione.<sup>45</sup> HPLC-grade methanol and acetonitrile, which were used as eluents in HPLC analysis, were purchased from Aldrich. The water used for solution and eluent preparations was Milli-Q pure water. Methylene chloride (certified A.C.S. spectranalyzed grade) used for the extractions was obtained from Fisher Scientific. High-purity  $\text{N}_2\text{O}$  gas was supplied by Mittler Supply Co. (South Bend, IN) and further filtered through a drying agent.

**$\gamma$ -Radiolysis.** When dilute aqueous solutions (<0.1 M) are irradiated with high-energy radiation (MeV), the energy is absorbed mainly by the solvent water, giving rise to the production of  $\bullet$ OH radicals, hydrated electrons, and H atoms as reactive free radicals and to some  $\text{H}_2\text{O}_2$ ,  $\text{H}_2$ , and  $\text{H}_3\text{O}^+$



where the numbers in parentheses indicate the  $G$  values (number of species transformed/100 eV;  $G = 1$  corresponds to  $1.036 \mu\text{MJ}^{-1}$ ).

The most convenient way to obtain almost totally oxidizing conditions during radiolysis is to saturate the solution with nitrous oxide, which converts the aqueous electrons to hydroxyl radicals:

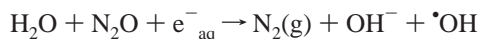


**TABLE 1: HPLC Gradient Program**

time (min)	0	3.5	18	20	29	35	45
30% methanol	100	85	60	50	50	100	100
acetonitrile	0	15	40	50	50	100	100

Under these conditions,  $G(\bullet\text{OH})$  is  $\sim 5.4$  and  $G(\text{H}^*)$  is  $\sim 0.55$  molecules/100 eV. In other words, about 90% of the radicals formed in the  $\text{N}_2\text{O}$ -saturated aqueous solutions are the  $\bullet\text{OH}$  radicals.

**Procedures.**  $\gamma$ -Radiolysis experiments for product studies were conducted in a Shepherd 109  $^{60}\text{Co}$  source and were repeated at least three times. The dose rate was  $\sim 14$  krad/min, as determined by Fricke dosimetry. Glass vials (Fisherbrand,  $19 \times 65 \text{ mm}^2$ ) were filled with 10 mL of quinoline solution (pH  $\sim 6$ ), sealed with rubber septa, and saturated with  $\text{N}_2\text{O}$  gas. To study the degradation over time, a sufficient number of samples were placed in the  $^{60}\text{Co}$  source to allow one to be taken out after different irradiation times for later HPLC analysis. When  $\text{K}_3\text{Fe}(\text{CN})_6$  was used, it was added after  $\text{N}_2\text{O}$  purging and just before the irradiation. Aluminum foil and amber vials were used to prevent any photooxidation reaction in room light. For the quantification of 8-hydroxyquinoline, vials containing 30 mL of  $\text{N}_2\text{O}$ -saturated quinoline solution were irradiated in a Shepherd 109  $^{60}\text{Co}$  source (14 krad/min dose rate). Immediately after the irradiation, 300  $\mu\text{L}$  of the internal standard (4-nitrophenol, 0.4 mM) was added to each vial. The aqueous solutions were extracted with  $3 \times 10 \text{ mL}$  of dichloromethane. The organic phase was concentrated (by flowing Ar above the solution) to around 1 mL before being injected into the GC. To determine the  $G$  values, four identical vials containing each 25 mL of quinoline solution,  $\text{N}_2\text{O}$ -saturated, were irradiated in a Shepherd 109  $^{60}\text{Co}$  source at a dose rate of 3 krad/min. The samples were irradiated such that less than 25% of the substrate was degraded and then analyzed by HPLC and GC-ECD.

**Analysis.** Identifications of the reaction products were first performed by HPLC by comparison of the retention times and the UV spectra (photodiode array detector) to those of the purchased or prepared standards. The HPLC system was a Hitachi D-7000 equipped with an L7200 autosampler and an L-7455 photodiode array detector. The reverse-phase columns used were an Alltech Hypersil BDS C18 3- $\mu\text{m}$  ( $150 \times 4.6 \text{ mm}^2$ ) column preceded by a Hypersyl BDS C18 5- $\mu\text{m}$  ( $7.5 \times 4.6 \text{ mm}^2$ ) guard column. A solvent gradient was used at a flow rate of 0.55 mL/min. The two eluents employed in the HPLC analysis were methanol (30% v/v) containing  $\sim 5 \text{ mM}$  tetraethyl- or tetra-*n*-propylammonium bromide (TEAB and TPAB) and acetonitrile. Both ion pair reagents were needed only when  $\text{K}_3\text{Fe}(\text{CN})_6$  was used. TPAB interfered with the detection of 4-hydroxyquinoline and quinoline-5,8-dione but helped achieve a good separation of 6-, 5- and 7-hydroxyquinolines. TEAB allowed good separation of 4-hydroxyquinoline and quinoline-5,8-dione but did not work out for the other compounds. The gradient program is described in Table 1. The monitoring wavelength was 234 nm.

The LCMS experiments were performed on a Micromass Quattro LC interfaced to a Waters Alliance LC having a photodiode array detector and autosampler. The same columns as in HPLC analysis were used. A solvent gradient was used at a flow rate of 0.55 mL/min. Because the TEAB and TPAB interfered with our analysis, the methanol eluent (30% v/v) was adjusted with formic acid such that the pH of this mobile phase was  $\sim 3$ . However, some peaks in our analysis could not be resolved, even when different gradients were tried. Electrospray (ES) mass spectra were acquired over the mass range of 50–650 at a rate of 1 s/scan.

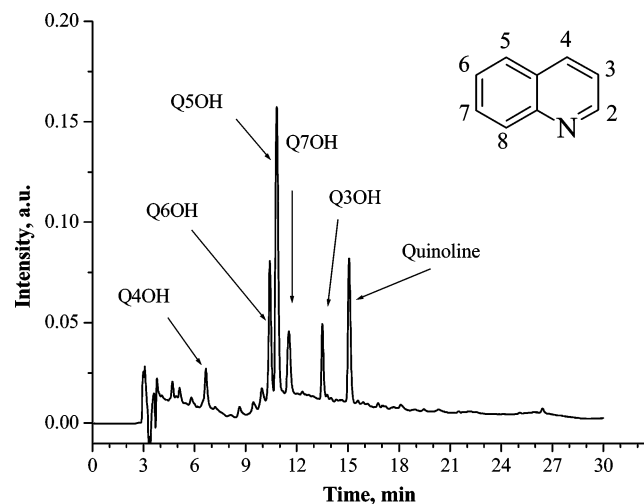


**Figure 1.** Chromatogram showing the separation of various mono-hydroxylated quinolines during the HPLC analysis. The retention time of 2-hydroxyquinoline is 12.5 min.

The presence of 8-hydroxyquinoline was first confirmed by using a solid-phase microextraction (SPME) fiber that was submerged in the irradiated aqueous solution for at least 40 min with stirring. The 65- $\mu\text{m}$  carbowax/divinylbenzene fiber was purchased from Supelco Chromatography. The fiber was then placed immediately into the GC/MS injector, which was kept at 220  $^{\circ}\text{C}$ . The EI analysis was carried out on a JEOL GC Mate interfaced to an HP 6890 GC. The column used was an HP-5 30 m  $\times$  0.32 mm i.d., 0.25- $\mu\text{m}$  film thickness. The column temperature program was 40  $^{\circ}\text{C}$  (2 min) to 90  $^{\circ}\text{C}$  (13  $^{\circ}\text{C}/\text{min}$ , hold 1 min) to 280  $^{\circ}\text{C}$  (13  $^{\circ}\text{C}/\text{min}$ , hold 10 min). The retention time and mass spectrum were compared to those of the standard.

For the quantification of 8-hydroxyquinoline, an HP 5890 II gas chromatograph with an ECD detector was used with a Restek Rtx-1 column (15 m  $\times$  0.32 mm, film thickness 1  $\mu\text{m}$ ). The inlet was kept at 180  $^{\circ}\text{C}$ , the detector was kept at 300  $^{\circ}\text{C}$ , and the column program was 60  $^{\circ}\text{C}$  (1 min) to 90  $^{\circ}\text{C}$  (20  $^{\circ}\text{C}/\text{min}$ , hold 10 min) to 140  $^{\circ}\text{C}$  (5  $^{\circ}\text{C}/\text{min}$ , hold 1 min) to 290 (20  $^{\circ}\text{C}/\text{min}$ , hold 8 min).

## Results and Discussion

**Product Analysis in  $\text{N}_2\text{O}$ -Saturated Solutions.** The first step in our study was to identify the monohydroxylated products formed in the degradation of quinoline under oxidative radiolytic conditions. Five out of the possible seven monohydroxylated quinolines (3-, 4-, 5-, 6-, and 7-hydroxyquinolines) were confirmed as the major identifiable products. No 2-hydroxyquinoline was observed in quantifiable amounts even though experiments with independently obtained standards show that it can be detected using the chosen analytical methods. The detection of 8-hydroxyquinoline was rather difficult under the present experimental conditions because it eluted at approximately the same time as the parent quinoline and exhibited a broad and long-tailed peak. Figure 1 shows a representative HPLC chromatogram of the reaction mixture following the  $\gamma$ -radiolysis of the quinoline solution. The presence of 8-hydroxyquinoline in the reaction mixture was separately confirmed by GC/MS using a solid-phase microextraction (SPME) procedure. Again, 2-hydroxyquinoline was not observed using this technique.

Quinoline is highly susceptible to attack by  $\cdot\text{OH}$ . Figure 2A shows the decay of quinoline during irradiation in the  $^{60}\text{Co}$  source. By fitting the decay to single-exponential decay kinetics, the lifetime for the degradation of quinoline under these

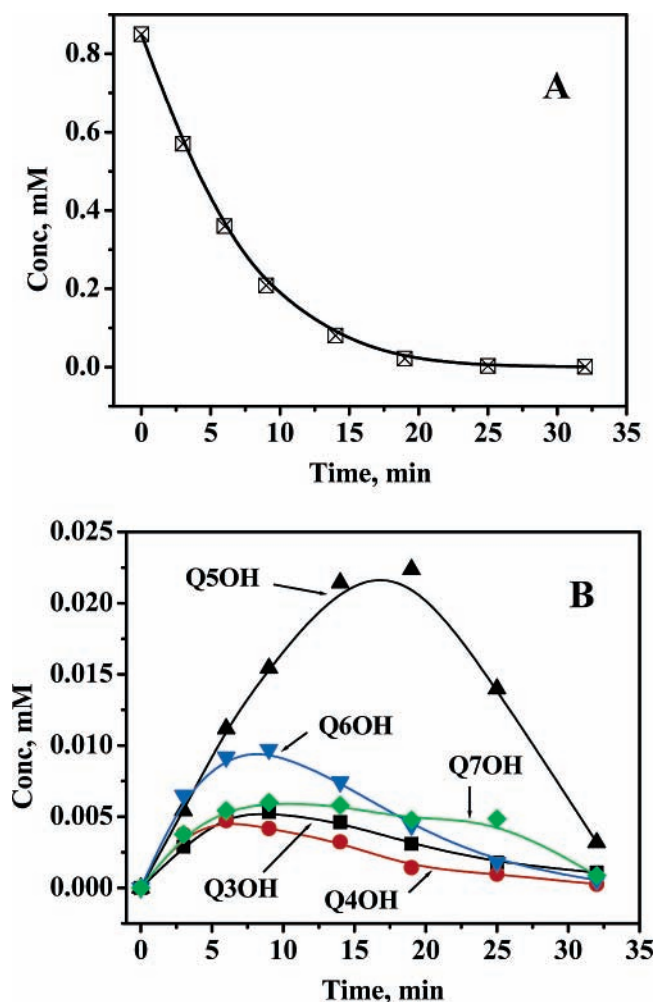


**Figure 2.** Degradation of an  $\text{N}_2\text{O}$ -saturated quinoline (0.8 mM) solution for a dose rate of 14 krad/min (A). Evolution and decay of the mono-hydroxylated products observed from HPLC analysis (B).

conditions (dose rate of 14 krad/min) was calculated to be  $\sim 9.24$  min. The evolution and the decay of the hydroxylated products as monitored in HPLC analysis are presented in Figure 2B. The difference in the growth pattern and their lifetime under radiolytic conditions show the complexity in elucidating the reaction mechanism of  $\cdot\text{OH}$ .

The comparison between the formation of 5-hydroxyquinoline and 8-hydroxyquinoline during the radiolysis of a 0.7 mM  $\text{N}_2\text{O}$ -saturated quinoline solution is shown in Figure 3.

The hydroxyl radical is an electrophilic species that has been shown to be selective toward addition and H atom abstraction reactions with heterocyclic compounds.<sup>27,46</sup> For example, the  $\cdot\text{OH}$  attack on pyridine occurred at the meta positions to an extent of 80% or more, as observed in ESR, pulse radiolysis, and product analysis.<sup>27,46</sup> No attack on the nitrogen (the site with the greatest electron density) was confirmed experimentally. In our study, the dominant products were expected to reflect the preferential attack of  $\cdot\text{OH}$  on the benzene ring. The pyridine ring is deactivated by the electronegativity of the nitrogen atom, especially at the C2 and C4 positions. However, all OH-substituted products except 2-hydroxyquinoline were observed in quantifiable amounts. From Figures 2 and 3, it is clear that the products formed by attack at the benzene ring are formed in higher concentration than the products formed by attack at the pyridine ring. Nevertheless, the formation of similar amounts of 3- and 4-hydroxylated quinolines would suggest that  $\cdot\text{OH}$  lacks the selectivity reported in other studies.<sup>27</sup> In addition to

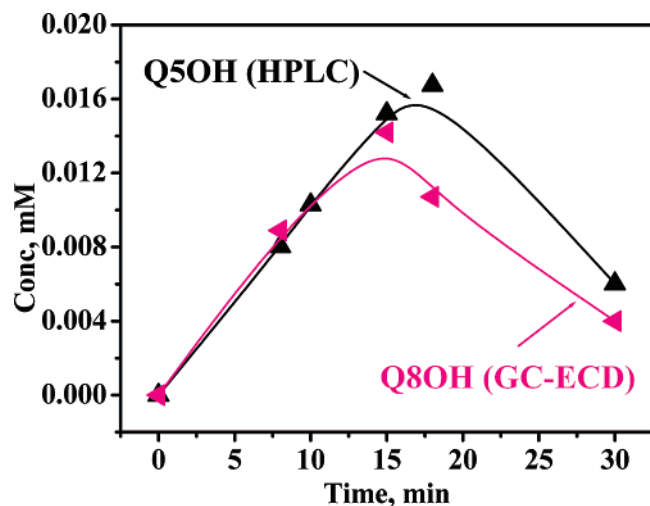
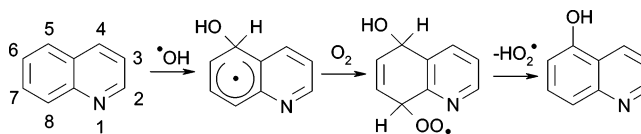


**Figure 3.** Formation of 5- and 8-hydroxyquinoline during the  $\gamma$ -radiolysis of a 0.7 mM  $N_2O$ -saturated quinoline solution (dose rate 14 krad/min).

these monohydroxylated quinolines, other products were also noted. During the  $\gamma$ -radiolysis of the aqueous quinoline solutions, settling of a brown powder was observed in the samples irradiated for extended times (more than 25 min). This indicated that higher-molecular-weight compounds with low solubility in water were formed during this process. The electrospray MS analysis (direct infusion) of the powder obtained by evaporating the water from a quinoline solution irradiated about 15 min is shown in Figure 4. Besides the MS signals corresponding to the monohydroxylated quinolines at  $m/z = 146$ , peaks indicating the formation of higher-molecular-weight species (e.g., a quinoline dimer with  $m/z = 257$ ) are observed, especially in the magnified part of the spectrum (shown in black). The peak corresponding to a molecular ion with  $m/z = 257$  was also observed during the LC/MS analysis. Because of the unavailability of the standards, identification or quantification of the compounds corresponding to the peaks was not possible.

These results are in disagreement with those of a previous study on the reaction of the hydroxyl radical with quinoline.<sup>42</sup>

#### SCHEME 1



Cermenati and co-workers<sup>42</sup> employed the photo-Fenton reaction to induce  $\bullet OH$ -mediated degradation of quinoline at pH 3. The major primary products identified in the photo-Fenton reaction were 5-hydroxyquinoline and 8-hydroxyquinoline, along with quinoline-5,8-dione as a secondary product. They proposed the mechanism shown in Scheme 1 to explain the formation of the hydroxylated products.

In the present study, the degradations were carried out in the absence of oxygen by saturating the solutions with nitrous oxide, and the natural pH of the solution was  $\sim 6$ . Along with 5- and 8-hydroxyquinoline as the major products, we also observed 3-, 6-, and 7-hydroxyquinolines. Traces of 6-hydroxyquinoline were reported in the photo-Fenton reaction, but 3- and 7-hydroxyquinoline were not observed.<sup>42</sup> This is quite surprising given that small amounts of 2- and 4-hydroxyquinolines (which would be formed by  $\bullet OH$  attack at the most deactivated positions in the pyridine ring) were reported by Cermenati et al.<sup>42</sup> The question arises as to how can one account for the differences between these two studies. Is it because of the different chemistry of the OH adducts (more specifically, that due to the presence/absence of oxygen or another oxidant) or the presence of a different species (e.g., an iron-oxo complex) that reacts in a different way with the quinoline? To get a better understanding of the mechanistic pathways of the reaction of  $\bullet OH$  with quinoline, we introduced  $K_3Fe(CN)_6$  as the additional oxidant, and its influence on the product distribution and yields was investigated.

**Product Analysis in  $\gamma$ -Radiolysis in the Presence of an Oxidant.** The formation of hydroxylated products with different isomer ratios is the result of different oxidation/disproportionation steps that follow the formation of the intermediate OH adducts. The possible degradation pathways for the OH adducts formed in the reaction of quinoline are presented in Scheme 2.

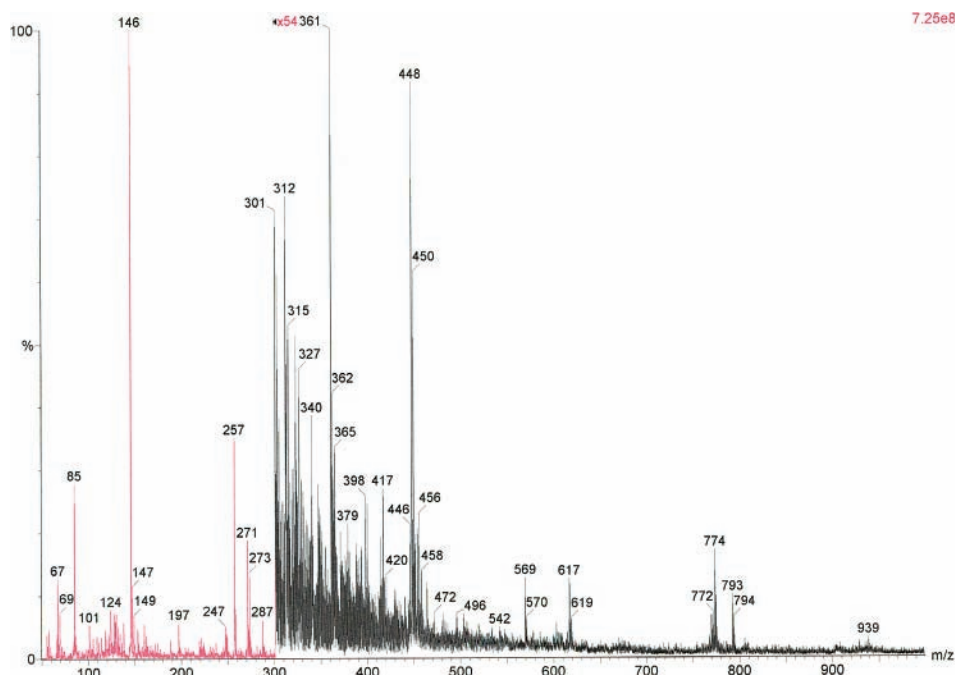
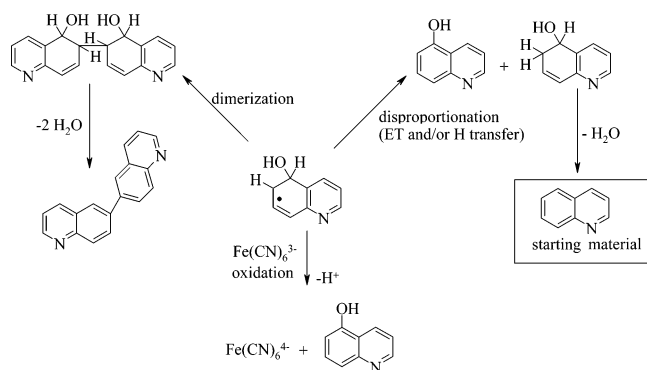


**Figure 4.** Mass spectrum of the powder formed in the  $\gamma$ -radiolysis experiments. (The black signal is magnified 54 times.)

## SCHEME 2

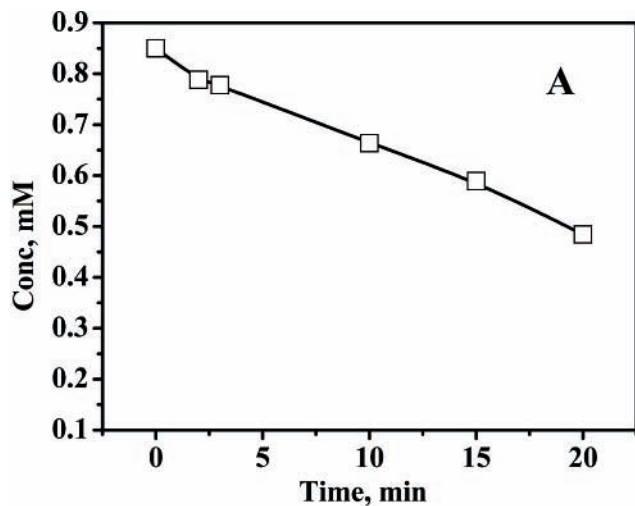


The presence of  $\text{K}_3\text{Fe}(\text{CN})_6$  ensures fast, quantitative conversion of the OH adducts to the final products and minimizes the contribution from the additional competing reactions, such as disproportionation or chain reactions. The decay of quinoline (0.85 mM) and the evolution of the products formed in the presence of 5 mM  $\text{K}_3\text{Fe}(\text{CN})_6$  are presented in Figure 5. As compared to the results shown in Figure 2A, the  $\cdot\text{OH}$ -induced decay of quinoline is relatively slow. When  $\text{K}_3\text{Fe}(\text{CN})_6$  was present in the solution, only about 50% of the quinoline was transformed in 20 min. However, the observed yields of most of the monohydroxylated quinolines were higher, and an additional product, quinoline-5,8-dione, was also formed (Figure 5B). This newly observed compound is a secondary product that is the result of the oxidation of the 5- and 8-hydroxyquinoline. No settling of the higher-molecular-weight product was observed in these experiments. This is an indication that the radical-induced polymerization of quinoline is suppressed in the presence of an oxidant.

The different concentrations of the monohydroxylated quinolines observed in the absence (Figure 2B) and in the presence of  $\text{K}_3\text{Fe}(\text{CN})_6$  (Figure 5B) demonstrate the importance of the chemistry of the OH adducts in the formation of the final products. Along with 5- and 8-hydroxyquinolines, 3-, 4-, 6-, and 7-hydroxylated quinolines are formed following the  $\cdot\text{OH}$  attack. The fact that no 2-hydroxyquinoline was observed when the fast conversion of the OH adducts was facilitated indicates again that the attack of  $\cdot\text{OH}$  at C2 may not be favored as compared to the attack of  $\cdot\text{OH}$  at the other quinoline positions. Surprisingly, this product was reported to be one of the products in the photo-Fenton reaction.<sup>42</sup> The disagreement between the results obtained in the presence of an additional oxidant ( $\text{K}_3\text{Fe}(\text{CN})_6$ ) and the photo-Fenton reaction suggests that different mechanistic pathways operate in the degradation of the quinoline. A detailed computational study of the  $\cdot\text{OH}$  attack at all of the different positions in quinoline provides further insight into the mechanistic aspects and is discussed in the second part of this study.<sup>52</sup>

**Radiolytic Yields (*G* Values).** The yields of the products and of quinoline after 6 min of irradiation of the  $\text{N}_2\text{O}$ -saturated aqueous quinoline solutions, reported as *G* values (number of molecules formed or destroyed per 100 eV), are presented in Table 2.

This is a quantitative way to compare the yields of products obtained when  $^{60}\text{Co}$  sources with different dose rates are used. The *G* value for the formation of the hydroxyl radical under these conditions is known to be  $G(\cdot\text{OH}) = 5.4$ . The *G* values for the disappearance of the quinoline and the formation of the monohydroxylated products were obtained after 6 min of irradiation at a dose rate of 3 krad/min with the molar concentration of  $\cdot\text{OH}$  produced per minute,  $\sim 15 \mu\text{M}$ . The



(a) Q3OH; (b) Q4OH; (c) Q5OH; (d) Q6OH; (e) Q7OH; (f) Q8OH; (g) 5,8-Q-dione

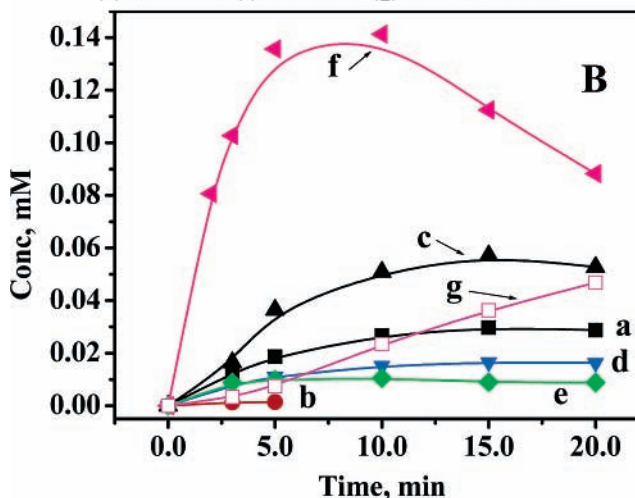


**Figure 5.** Degradation of an  $\text{N}_2\text{O}$ -saturated quinoline (0.85 mM) solution (A) and the evolution of the products (B) in the presence of 5 mM  $\text{K}_3\text{Fe}(\text{CN})_6$ . The dose rate is 14 krad/min.

similarity between the *G* value of quinoline disappearance and  $G(\cdot\text{OH})$  suggests a quantitative attack by the  $\cdot\text{OH}$  radicals. However, in the present case, there is a discrepancy between the amount of quinoline degraded and the amount of monohydroxylated compounds formed after the same irradiation time, indicating that the monohydroxylated quinolines constitute only a fraction of the total mass balance. The yields of the monohydroxylated products are significantly lower than  $G(\cdot\text{OH}) = 5.4$  or the  $G(-\text{Q}) = 5.21$ . Such a discrepancy is not an unusual phenomenon.<sup>27,47-49</sup> In the reaction of  $\cdot\text{OH}$  with 2'-deoxyguanosine, the pulse radiolysis studies account for the reactivity of about 80% of the hydroxyl radicals,<sup>50</sup> whereas the final product analysis accounted for only 25% of the hydroxyl radicals.<sup>51</sup> A study of the reactivity of  $\cdot\text{OH}$  with pyridine reported significantly lower yields of the three isomeric hydroxypyridines following the radiolysis of  $\text{N}_2\text{O}$ -saturated solutions (0.13 for 3-hydroxypyridine, 0.4 for 2-hydroxypyridine, and 0.20 for 4-hydroxypyridine).<sup>27</sup> Similarly, Mark and co-workers<sup>48</sup> reported  $G(\text{phenol}) \approx 0.5$  and  $G(\text{biphenyl}) \approx 1.7-1.8$  in the radiolysis of benzene in the absence of  $\text{O}_2$ . These studies suggest that the formation of dimers and/or of higher-molecular-weight compounds is an important process. The results obtained in the present study are in agreement with these findings.

**TABLE 2: G Values for the Disappearance of the Quinoline and Formation of Monohydroxylated Quinolines during the Radiolysis of N<sub>2</sub>O-Saturated Aqueous Quinoline Solutions**

compounds	-Q	Q2OH	Q3OH	Q4OH	Q5OH	Q6OH	Q7OH	Q8OH
G values	-5.21 ± 0.28		0.05 ± 0.007	0.06 ± 0.002	0.09 ± 0.001	0.11 ± 0.005	0.064 ± 0.002	0.085 ± 0.005

**TABLE 3: G Values for the Disappearance of the Quinoline and Formation of Monohydroxylated Quinolines during the Radiolysis of N<sub>2</sub>O-Saturated Aqueous Quinoline Solutions Containing K<sub>3</sub>Fe(CN)<sub>6</sub>**

compounds	-Q	Q5,8-dione	Q3OH	Q4OH	Q5OH	Q6OH	Q7OH	Q8OH
G value, 5mM Fe(CN) <sub>6</sub> <sup>3-</sup>	-4.54 ± 0.29	0.023 ± 0.0002	0.24 ± 0.009	0.034 ± 0.0004	0.68 ± 0.032	0.17 ± 0.0015	0.17 ± 0.012	1.4 ± 0.15

The *G* values for the destruction of quinoline and formation of the products upon addition of 5 mM K<sub>3</sub>Fe(CN)<sub>6</sub> are presented in Table 3. The *G* values of all but one product (4-hydroxyquinoline) are altered as compared to those obtained in the absence of K<sub>3</sub>Fe(CN)<sub>6</sub>. The *G* value of 4-hydroxyquinoline decreased in the presence of Fe(CN)<sub>6</sub><sup>3-</sup>. According to these measurements, the monohydroxylated quinolines are formed as expected by the attack at C3 and the benzene ring carbons.

**Mechanistic Aspects.** It is postulated that the final hydroxylated products are formed during  $\gamma$ -radiolysis by the disproportionation of the OH adducts.<sup>1</sup> Regarding the disproportionation reaction, it is unclear whether it proceeds through an electron transfer followed by proton transfer or a hydrogen atom transfer. For each molecule of the hydroxylated product, two molecules of •OH are being consumed. If the dehydration reaction with the formation of the starting material occurs, then only the transformation of one molecule of quinoline is responsible for the formation of one molecule of the hydroxylated product. The discrepancy between *G*(Q) and *G*(hydroxylated products) shown in Table 2 indicates that this is not the dominant reaction channel. Moreover, the real *G* value for the degradation of quinoline should be adjusted for the disproportionation reaction of the OH adducts that leads to the formation of the starting material. As shown in Scheme 2, one molecule of quinoline is regenerated for every molecule of hydroxylated product during the disproportionation reaction. This discrepancy of the *G* values would strongly support an additional reaction channel for the degradation of quinoline, like a chain-type reaction. The dimerization pathway is supported by the MS results. However, the observation of additional MS peaks, corresponding to high-molecular-weight compounds, along with the *G* value for the destruction of quinoline, suggests the involvement of the parent compound in more complex reactions. The difference in the growth pattern and the lifetime of the monohydroxylated products under radiolytic conditions further demonstrates the complexity of the reaction pathways. The *G* values, calculated at the beginning of the reaction when the interference of additional competing reactions was considered minimal, support this. For example, it is 6-hydroxyquinoline that shows the greatest *G* value at earlier times in Table 2, but it is 5-hydroxyquinoline that is formed in the highest concentration over the course of the reaction. When K<sub>3</sub>Fe(CN)<sub>6</sub> was used to get a “snapshot” of the reactivity of the hydroxyl radical, the *G* values and the observed product concentrations correlate well. Under these conditions, 8-hydroxyquinoline has the highest *G* value and is considered to be the dominant product.

It is clear that the chemistry of the OH adducts plays an important role in the outcome of this reaction. The results obtained in the radiolysis of quinoline are different than those obtained during the photo-Fenton degradation, even in the presence of an additional oxidant. This suggests that the nature of the steady-state products depends strongly on the first step of the reaction (e.g., the •OH attack), whereas the distribution of the products is dictated by the reactivity of the OH adducts.

It is very important and desirable to get a clear understanding of the weight of each step toward the outcome of the net reaction in general. This understanding will provide the possibility to manipulate the chemical transformations in each step of the reaction to get a desired outcome. The computational investigation of the •OH attack at all carbon positions in quinoline is presented in the second part of this investigation.<sup>52</sup>

**Acknowledgment.** We thank Dr. Bill Boggess at the ND Mass Spectrometry Facility for all of his help during the MS analysis and Dr. Dan Meisel for helpful discussions. Special thanks to the ND Center for Environmental Science and Technology (CEST) for the use of the analytical facilities and to Mr. Dennis Birdsell for his assistance in using the instrumentation. This work was supported by the Office of Basic Energy Sciences of the U.S. Department of Energy. This is contribution no. NDRL-4563 from the Notre Dame Radiation Laboratory.

## References and Notes

- (1) von Sonntag, C. *The Chemical Basis of Radiation Biology*; Taylor & Francis: London, 1987.
- (2) Foote, C. S. *Active Oxygen in Chemistry*; Blackie Academic & Professional: London, 1995.
- (3) Cooper, W. J.; Curry, R. D.; O'Shea, K. E. *Environmental Applications of Ionizing Radiation*; John Wiley & Sons: New York, 1998.
- (4) Motta, F.; Ghigo, G.; Tonachini, G. *J. Phys. Chem. A* **2002**, *106*, 4411–4422.
- (5) Dibble, T. S. *J. Am. Chem. Soc.* **2001**, *123*, 4228–4234.
- (6) Barckholtz, C.; Barckholtz, T. A.; Hadad, C. M. *J. Phys. Chem. A* **2001**, *105*, 140–152.
- (7) Marusawa, H.; Ichikawa, K.; Narita, N.; Murakami, H.; Ito, K.; Tezuka, T. *Bioorg. Med. Chem.* **2002**, *10*, 2283–2290.
- (8) Rosen, G. M.; Tsai, P.; Barth, E. D.; Dorey, G.; Casara, P.; Spedding, M.; Halpern, H. J. *J. Org. Chem.* **2000**, *65*, 4460–4463.
- (9) Bard, A. J.; Fox, M. A. *Acc. Chem. Res.* **1995**, *28*, 141–145.
- (10) Halpern, H. J.; Yu, C.; Barth, E.; Peric, M.; Rosen, G. M. *P Natl. Acad. Sci. U.S.A.* **1995**, *92*, 796–800.
- (11) Peller, J.; Wiest, O.; Kamat, P. V. *J. Phys. Chem. A* **2004**, *108*, 10925–10933.
- (12) Atkinson, R.; Aschmann, S. M. *Int. J. Chem. Kinet.* **1994**, *26*, 929–944.
- (13) Kwok, E. S. C.; Harger, W. P.; Arey, J.; Atkinson, R. *Environ. Sci. Technol.* **1994**, *28*, 521–527.
- (14) Andino, J. M.; Smith, J. N.; Flagan, R. C.; Goddard, W. A.; Seinfeld, J. H. *J. Phys. Chem.* **1996**, *100*, 10967–10980.
- (15) Ghigo, G.; Tonachini, G. *J. Am. Chem. Soc.* **1999**, *121*, 8366–8372.
- (16) Pelizzetti, E.; Minero, C.; Piccinini, P.; Vincenti, M. *Coord. Chem. Rev.* **1993**, *125*, 183–193.
- (17) Adewuyi, Y. G. *Ind. Eng. Chem. Res.* **2001**, *40*, 4681–4715.
- (18) Kamat, P. V. *Chem. Rev.* **1993**, *93*, 267–300.
- (19) Ames, B. N.; Shigenaga, M. K. *Ann. N.Y. Acad. Sci.* **1992**, *663*, 85–96.
- (20) Stadtman, E. R. *Science* **1992**, *257*, 1220–1224.
- (21) Ames, B. N.; Shigenaga, M. K.; Hagen, T. M. *P Natl. Acad. Sci. U.S.A.* **1993**, *90*, 7915–7922.
- (22) Malins, D. C.; Polissar, N. L.; Gunselman, S. J. *P Natl. Acad. Sci. U.S.A.* **1996**, *93*, 2557–2563.
- (23) Kaur, H.; Halliwell, B. *Anal. Biochem.* **1994**, *220*, 11–15.
- (24) Halliwell, B.; Kaur, H. *Free Radical Res.* **1997**, *27*, 239–&.
- (25) Walling, C.; Johnson, R. A. *J. Am. Chem. Soc.* **1975**, *97*, 363–367.

- (26) Eberhardt, M. K. *J. Phys. Chem.* **1975**, *79*, 1913–1916.
- (27) Selvarajan, N.; Raghavan, N. V. *J. Phys. Chem.* **1980**, *84*, 2548–2551.
- (28) Fenton, H. J. H. *J. Chem. Soc.* **1894**, *65*, 899–910.
- (29) Hage, J. P.; Llobet, A.; Sawyer, D. T. *Bioorg. Med. Chem.* **1995**, *3*, 1383–1388.
- (30) Sawyer, D. T.; Sobkowiak, A.; Matsushita, T. *Acc. Chem. Res.* **1996**, *29*, 409–416.
- (31) Wardman, P.; Candeias, L. P. *Radiat. Res.* **1996**, *145*, 523–531.
- (32) Goldstein, S.; Meyerstein, D. *Acc. Chem. Res.* **1999**, *32*, 547–550.
- (33) Pogożelski, W. K.; Mcneese, T. J.; Tullius, T. D. *J. Am. Chem. Soc.* **1995**, *117*, 6428–6433.
- (34) Buda, F.; Ensing, B.; Gribnau, M. C. M.; Baerends, E. J. *Chem.—Eur. J.* **2001**, *7*, 2775–2783.
- (35) Bray, W. C.; Gorin, M. H. *J. Am. Chem. Soc.* **1932**, *54*, 2124–2125.
- (36) Henle, E. S.; Luo, Y. Z.; Linn, S. *Biochemistry* **1996**, *35*, 12212–12219.
- (37) Luo, Y. Z.; Henle, E. S.; Linn, S. *J. Biol. Chem.* **1996**, *271*, 21167–21176.
- (38) Goldstein, S.; Czapski, G.; Rabani, J. *J. Phys. Chem.* **1994**, *98*, 6586–6591.
- (39) Theruvathu, J. A.; Aravindakumar, C. T.; Flyunt, R.; von Sonntag, J.; von Sonntag, C. *J. Am. Chem. Soc.* **2001**, *123*, 9007–9014.
- (40) Stafford, U.; Gray, K. A.; Kamat, P. V. *J. Phys. Chem.* **1994**, *98*, 6343–6351.
- (41) Collin, G.; Hoke, H. In *Ullmann's Encyclopedia of Industrial Chemistry*; Gerhartz, W., Yamamoto, S. Y., Campbell, F. T., Pfefferkorn, R., Rounsaville, J. F., Russey, W., Eds.; VCH: Weinheim, Germany, 1993; Vol. A22, pp 465–469.
- (42) Cermenati, L.; Pichat, P.; Guillard, C.; Albin, A. *J. Phys. Chem. B* **1997**, *101*, 2650–2658.
- (43) Nicolaescu, A. R.; Wiest, O.; Kamat, P. V. *J. Phys. Chem. A* **2003**, *107*, 427–433.
- (44) Cragoe, E. J.; Robb, C. M. *Org. Synth.* **1969**, *CV 5*, 635.
- (45) Pratt, Y. T.; Drake, N. L. *J. Am. Chem. Soc.* **1960**, *82*, 1155–1161.
- (46) Steenken, S.; O'Neill, P. *J. Phys. Chem.* **1978**, *82*, 372–374.
- (47) Eberhardt, M. K.; Yoshida, M. *J. Phys. Chem.* **1973**, *77*, 589–597.
- (48) Mark, G.; Schuchmann, H. P.; Schuchmann, M. N.; Prager, L.; Von Sonntag, C. *Environ. Sci. Technol.* **2003**, *37*, 372–378.
- (49) Prager, L.; Mark, G.; Matzing, H.; Paur, H. R.; Schubert, J.; Frimmel, F. H.; Hesse, S.; Schuchmann, H. P.; Schuchmann, M. N.; Von Sonntag, C. *Environ. Sci. Technol.* **2003**, *37*, 379–385.
- (50) Candeias, L. P.; Steenken, S. *Chem.—Eur. J.* **2000**, *6*, 475–484.
- (51) Berger, M.; Cadet, J. *Z. Naturforsch., B* **1985**, *40*, 1519–1531.
- (52) Nicolaescu, A. R.; Wiest, O.; Kamat, P. V. *J. Phys. Chem. A* **2005**, *109*, 2829.